

Article

Tribological Behavior of GTL Base Oil Improved by Ni-Fe Layered Double Hydroxide Nanosheets

Shuo Xiang ¹ , Xinghao Zhi ², Hebin Bao ^{1,*}, Yan He ^{1,*}, Qinhui Zhang ¹, Shigang Lin ¹, Bo Hu ¹, Senao Wang ¹, Peng Lu ³, Xin Yang ¹, Qiang Tian ⁴ and Xin Du ¹

¹ Army Logistics Academy of PLA, Chongqing 401331, China; xslaplace@163.com (S.X.); 15223276757@163.com (Q.Z.)

² Unit 326587, Jinzhou 121001, China; zhx052887@163.com

³ Unit 91967, Xingtai 054001, China

⁴ Chengdu Quality Supervision Station of PLA, Chengdu 610041, China

* Correspondence: baohb@vip.163.com (H.B.); 18623006256@163.com (Y.H.)

Abstract: The layered double hydroxide (LDH) has been practically applied in the field of tribology and materials science due to its unique physicochemical properties, weak bonding, flexible structural composition, and adjustable interlayer space. In this work, a series of ultrathin and flexible composition of Ni-Fe LDH samples were prepared via a cost-effective room-temperature co-precipitation process. Then, they were mechanically dispersed into GTL base oil and their lubricating performance were tested by a four-ball tribometer. It is found that the variation of Ni-Fe ratio of Ni-Fe LDH has a great influence on the improvement of lubricating performance of GTL base oil. At the same concentration (0.3 mg/mL), the Ni-Fe LDH with Ni/Fe ratio of 6 was demonstrated to exhibit the best lubricating performance and the AFC, WSD, the wear volume, surface roughness and average wear scar depth decreased 51.3%, 30.8%, 78.4%, 6.7% and 50.0%, respectively. SEM-EDS and X-ray photoelectron spectra illustrated that the tribo-chemical film consisting of iron oxides and NiO with better mechanical properties formed and slowly replaced the physical film, which resists scuffing and protect solid surface from severe collisions.

Keywords: gas to liquid; lubricating oil; lubricating performance; layered double hydroxide



Citation: Xiang, S.; Zhi, X.; Bao, H.; He, Y.; Zhang, Q.; Lin, S.; Hu, B.; Wang, S.; Lu, P.; Yang, X.; et al. Tribological Behavior of GTL Base Oil Improved by Ni-Fe Layered Double Hydroxide Nanosheets. *Lubricants* **2024**, *12*, 146. <https://doi.org/10.3390/lubricants12050146>

Received: 27 February 2024

Revised: 2 April 2024

Accepted: 10 April 2024

Published: 26 April 2024



Copyright: © 2024 by the authors. Licensee MDPI, Basel, Switzerland. This article is an open access article distributed under the terms and conditions of the Creative Commons Attribution (CC BY) license (<https://creativecommons.org/licenses/by/4.0/>).

1. Introduction

Friction and wear are widely used in the chemical industry, aerospace, machinery manufacturing, transportation, metallurgy, oceanography, bioengineering, renewable energy and daily life [1–5]. Along with the development of modern industry, friction and wear not only cause energy loss and mechanical failure, but also metal corrosion and environmental pollution [6,7]. To address these problems, lubricants are utilized extensively and have been proven as an efficient means of minimizing friction and wear in the fields of transportation, metal cutting, mining, construction, power generation, power transmission, and so on [8,9]. Modern commercial lubricants can be grouped as lubricating oils, lubricating greases, solid lubricants and compressed air or other gases, and the first one accounts for about 80% of them [10]. Lubricating oil is generally composed of two parts, a base oil and an additive. The former is the primary component of lubricating oil and typically makes up the majority of its composition (usually 70–95%), which determines the basic properties of lubricating oil [11].

With the progression of contemporary economy and technology, friction and wear not only culminate in energyipation and mechanical malfunction, also instigate metal corrosion and environmental contamination [6]. To address these predicaments, lubricants are extensively employed and have been substantiated as an efficacious means of minimizing friction and wear in the realms of transportation, metal cutting, mining, construction, power generation, power transmission, and so forth [8,9]. Modern commercial

lubricants can be categorized as lubricating oils, lubricating greases, solid lubricants, and compressed air or other gases, wherein the former constitutes approximately 80% of the aforementioned [10]. Lubricating oil is generally comprised of two constituents, namely a base oil and an additive. The former serves as the principal component of lubricating oil and predominantly constitutes its composition (usually 70–95%), thereby determining the fundamental properties of the lubricating oil [11]. As a synthetic product produced from natural gas using the Fischer-Tropsch process, gas to liquid (GTL) base oil have excellent characteristics, including ultra-high VIs ($VI > 140$), originally no sulphur and nitrogen, very low evaporative losses and inappreciable aromatic content [12]. In light of this, GTL base oil is a promising and environmentally friendly alternative to traditional mineral base oil, which contains nitride and sulfide. Additives can compensate and improve the lubricating properties of base oils. Over the past decades, extensive research has been conducted on various forms of additives such as composites, nanoparticles, liquids and two-dimensional (2D) materials. Among them, 2D materials are expected to be an alternative to liquid lubricant additives due to their high specific surface area, chemical stability, and continuous formation of protective films on friction surfaces. Due to the characteristics of high specific surface area, remarkable chemical stability, and the ability to continuously form a protective film on the friction surface, a variety of two-dimensional (2D) materials have been extensively studied in the field of tribology, including graphene [13,14], black phosphorus (BP) [15,16], h-BN [17,18], MoS₂ [19–21], WS₂ [22,23], MXene [24–26], and layered double hydroxides (LDHs) [27,28]. As with other 2D materials, the synthesis strategies for layered double hydroxide nanosheets can be divided into two main categories: bottom-up direct synthesis processes and top-down exfoliation processes. Various bottom-up strategies have been developed for the direct preparation of LDHs from suitable precursors, including hydrothermal, co-precipitation, microemulsion, sol-gel, and reconstruction methods, through which LDHs with tunable dimensions, thicknesses, crystallinity, and shapes have been prepared. The top-down exfoliation process usually involves swelling/interpolation to enlarge the interlayer distance, followed by exfoliation of bulk LDHs. From the synthesis of the LDHs are indeed suitable candidates for tribological applications from the point of view of simplicity of process, flexibility of control and low cost [2,29]. More importantly, LDHs are environmentally friendly materials that meet the requirements of sustainable development, and have become potential environmentally friendly lubricant additives, replacing traditional lubricant additives, such as zinc dialkyl dithiophosphate (T202), isobutylene sulphide (T308), di-n-butyl phosphite (T304), chlorinated paraffin wax (T301), and molybdenum dithiocarbamate (MoDTC), etc.

In the present article, a series of ultrathin and flexible composition of Ni-Fe LDH samples were produced via a cost-effective room-temperature co-precipitation process. The obtained Ni-Fe LDH samples were characterized by various tools such as powder X-ray diffraction (XRD), Fourier transform infrared (FT-IR) spectroscopy, thermogravimetric/differential thermal analysis (TG/DTA). The anti-wear and friction-reducing properties of the as-synthesized Ni-Fe LDH samples in GTL base oil were systematically studied by a four-ball tribometer. White light interferometer (WLI) methods were applied to analyze the wear surface. The composition and microstructure of the tribo-chemical film were analyzed by scanning electron microscope, energy dispersion spectrum (SEM-EDS), and X-ray photoelectron spectroscopy (XPS). The lubrication mechanism of GTL base oil improved by Ni-Fe LDH was presented. The lubrication mechanism of Ni-Fe LDH in GTL base oil was further discussed.

2. Materials and Methods

2.1. Materials

Sodium bicarbonate (NaHCO₃), nickel nitrate hexahydrate (Ni(NO₃)₂·6H₂O), iron nitrate nonahydrate (Fe(NO₃)₃·9H₂O), methyl alcohol (CH₃OH), methyl alcohol (CH₃CH₂OH), and petroleum ether (90–120 °C) were of analytical grade and purchased from Shanghai Aladdin Biochemical Technology Co., Ltd. (Shanghai, China). The Risella X 430 base oil

(GTL 430) supplied by Shell was used as fluid lubricant to formulate dispersions (Typical characteristics showed in Table 1). All chemicals were used as received without further purification and distilled water was used during all experiments.

Table 1. Typical characteristics of the Risella X 430 base oil (GTL 430).

Test Description	Result	Method
Kinematic viscosity (mm ² /s) (40 °C)	44.23	ASTM D445
Kinematic viscosity (mm ² /s) (100 °C)	7.62	ASTM D445
Viscosity Index	140	ASTM D2270
Appearance	Clear to bright	Visual
Colour saybolt	30	ASTM D156
Colour (ASTM) (Quantitative)	0.50	ASTM D1500
Density (kg/m ³) (15 °C)	827.70	ASTM D4052
Refractive index (20 °C)	1.46	ASTM D1218
Pour point (°C)	−45	ASTM D6749
Flash point (°C) (PMcc)	234	ASTM D93

2.2. Sample Preparation

Ni(NO₃)₂·6H₂O, urea, Fe(NO₃)₃·9H₂O and TEA were added into a 200 mL solution using deionized water such that their typical concentrations were 7.5 mM, 2.5 mM, 17.5 mM and 10 mM. A magnetic stir bar was added to the flask and the resulting solution was stirred at 300 rpm for 24 h at room temperature. The reaction mixture was heated to reflux at 100 °C with continuous stirring in a silicone oil bath for 48 h. Subsequently, the system was cooled to room temperature in the air. The dispersion was centrifuged at 3000 rpm for 10 to 15 min at room temperature to separate the precipitate from the solvent. The precipitate was then washed three times with deionized water by shaking and then centrifuging to separate. The clean precipitate was then redispersed in isopropanol with an additional two washing steps. The as-produced platelets were subsequently tip-sonicated for 1 h using a Fischer Scientific Sonic Dismembrator Ultrasonic Processor at 40% power at a frequency of 37 kHz (with Fisher Scientific Isotemp refrigerated bath circulator cooling system held at 5 °C). Further modification of the solid lubricant is necessary for stable dispersion in lubricating oils. Ni-Fe LDH powders were added to an ethanol solution containing 15 wt.% oleic acid and sonicated for 30 min. The resulting mixture was then dried to obtain the modified powder. The 0.wt.%, 0.1 wt.%, 0.2 wt.%, 0.3 wt.%, 0.4 wt.%, 0.5 wt.% modified powders were then added to GTL 430 and dispersed for 30 min using an ultrasonic immersion probe sonicator.

2.3. Characterization of Ni-Fe LDH

The as synthesized Ni-Fe LDH powders were characterized by using different analysis techniques. The crystal structure of Ni-Fe LDH powders was recorded using a powder X-ray diffraction (XRD, Bruker D8 ADVANCE, Karlsruhe, Germany) with Cu K α radiation in the 2 θ range from 5° to 90° and scan step 0: 02°. The infrared spectroscopy of Ni-Fe LDH powders was performed on Fourier transform infrared spectroscopy (FT-IR PerkinElmer Spectrum, Shelton, CT, USA) at a resolution of 4 cm^{−1}. Thermal stability of Ni-Fe LDH powders was evaluated using thermogravimetric analysis instrument (TG/DSC, SDT-Q600, TA Instruments, New Castle, DE, USA) under pure N₂ flow (100 mL min^{−1}) to study the weight changes with temperature. The samples were heated from room temperature to 850 °C at a heating rate of 10 °C/min.

2.4. Tribological Experiments and Evaluation

The friction and wear properties of the lubricant were examined on an SHM-1A four-ball tester (Jinan Shunmao test instrument Co., Ltd., Jinan, China) with a rotational speed of 1200 rpm, pressure loads of 200 N, 300 N, 400 N, 500 N, and 600 N, and a test time of 1 h at room temperature. Before friction test, the steel balls were successively ultrasonicated in

acetone and anhydrous ethanol to remove a wide variety of contaminants on the surface, then washed with deionized water and dried in a nitrogen atmosphere. For each friction test, 100 mL of lubricant was added to the contact area of the ball friction pair to ensure that the friction pair was lubricated throughout the sliding process.

In order to obtain accurate and reliable tribological data, each set of experiments was repeated three times and the coefficient of friction of the friction tester was recorded with an accuracy of ± 0.01 . All the tests were carried out in humid air at room temperature and relative humidity of 30–50%. The parameters of the tested steel balls are shown in Table 2.

Table 2. Experimental parameters and basic characteristics of the steel balls used.

Parameter	GTL 430	0.1 mg/mL Ni-Fe LDH	0.2 mg/mL Ni-Fe LDH	0.3 mg/mL Ni-Fe LDH	0.4 mg/mL Ni-Fe LDH	0.5 mg/mL Ni-Fe LDH
Speed	1200 rpm	1200 rpm	1200 rpm	1200 rpm	1200 rpm	1200 rpm
	200 N	-	-	-	-	-
	300 N	-	-	-	-	-
Load	400 N	-	-	-	-	-
	500 N	-	-	-	-	-
	600 N	600 N	600 N	600 N	600 N	600 N
Temperature	RT	RT	RT	RT	RT	RT
Test Duration	60 min	60 min	60 min	60 min	60 min	60 min
Component	Elastic modulus (MPa)		Poisson ratio	Diameter	Rockwell	Surface roughness
GCr15	2.085×10^5		0.3	12.7 mm	60 ± 1	$0.256 \mu\text{m}$

To explore the friction mechanism of the Ni-Fe LDH, the morphology of the worn surface was observed using a JEOL JSM-6610LV scanning electron microscope (JEOL, Tokyo, Japan) and a white light interferometer (WLI) with a Contour GT-X 3D optical profiler (Bruker, Karlsruhe, Germany), and the elemental distribution and composition of the worn surface was identified and quantified using an Oxford X-Max 20 mm² energy dispersive X-ray spectrometer (Oxford Instruments, Oxford, UK). In order to further determine the elemental composition and chemical state of the ternary films on the worn surfaces, X-ray photoelectron spectroscopy replication (XPS) tests were carried out using an ESCALAB 250Xi X-ray photoelectron spectrometer (Bruker, Karlsruhe, Germany) to probe the deposition of the ternary films.

3. Results and Discussion

3.1. Material Characterization

As can be seen from the XRD pattern of the Ni-Fe LDH powders with various Ni/Fe ratio (Figure 1a,b), the characteristic diffraction peaks of the as-prepared samples at 11.3° , 22.7° , 34.4° , 38.9° , and 60.1° corresponded to the (003) (006), (012) (015), and (110) crystal planes of NiFe-LDHs (PDF#40–0215), respectively, indicating that these samples have typical hydrotalcite-like crystal structure [27]. Most noteworthy, the XRD patterns of the samples with smaller Ni-Fe ratio (2:1, 3:1) displayed sharper and narrower peaks, implying higher degrees of crystallinity increase [2]. All the characteristic peaks of the LDH structure appeared in the XRD pattern of the samples can be well indexed to the characteristic Ni-Fe LDH structure (JCPDS no. 40-0215), conforming the successful preparation of NiFe-LDHs.

The FT-IR spectra of the Ni-Fe LDHs are shown in Figure 1c. The infrared bands around 3500 cm^{-1} corresponds to the OH-stretching vibration and the one at 1627 cm^{-1} is attributed to the H-O-H deformation, which are the evidence of the hydration of the LDH samples. The peak located at 1341 cm^{-1} , which originates from the ν stretching vibration of the NO_3 groups in the LDH interlayer. Bands under 1000 cm^{-1} can be ascribed to bonds between O and metallic atoms forming the hydroxide layers.

Figure 2 displays the TG and DTG curves. The DTG curve exhibited endothermic peaks at a temperature lower than 100°C , which could be related to the release of absorbed H_2O molecules. The endothermic peaks at the temperature range of $200\text{--}500^\circ\text{C}$ are believed

to result from the dissipation of -OH groups in the Ni-Fe LDH. Accordingly, assuming that the dissipation of interlayer H₂O molecules occurred at the temperature range of 100–200 °C, the H₂O content in the interlayer was calculated from the weight loss of 5.4% which occurred between 100 °C and 200 °C.

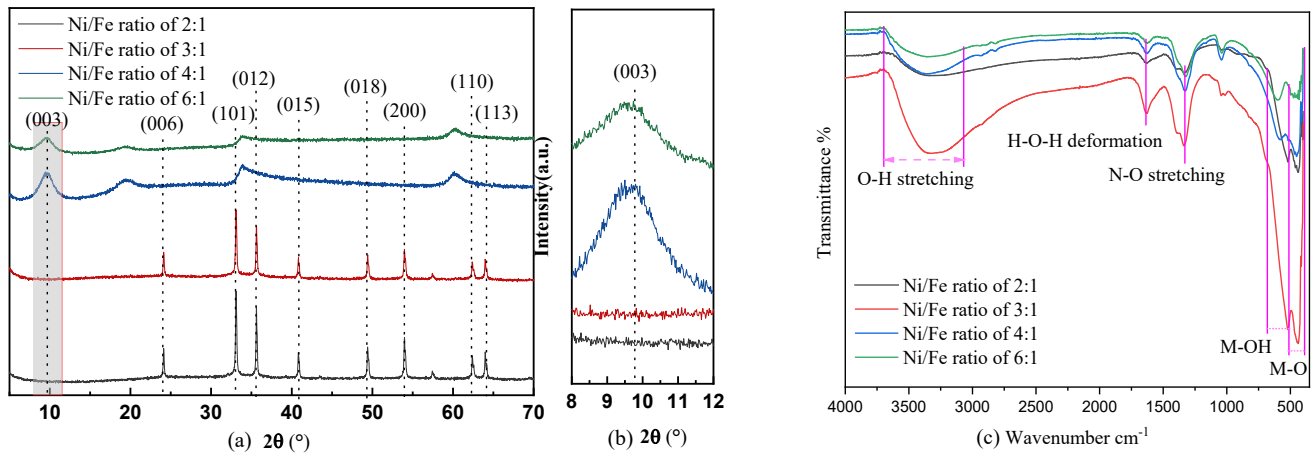


Figure 1. The powder X-ray patterns of the four as-prepared Ni-Fe LDH samples (a,b). FTIR measurement of the four synthesized Ni-Fe LDH samples (c).

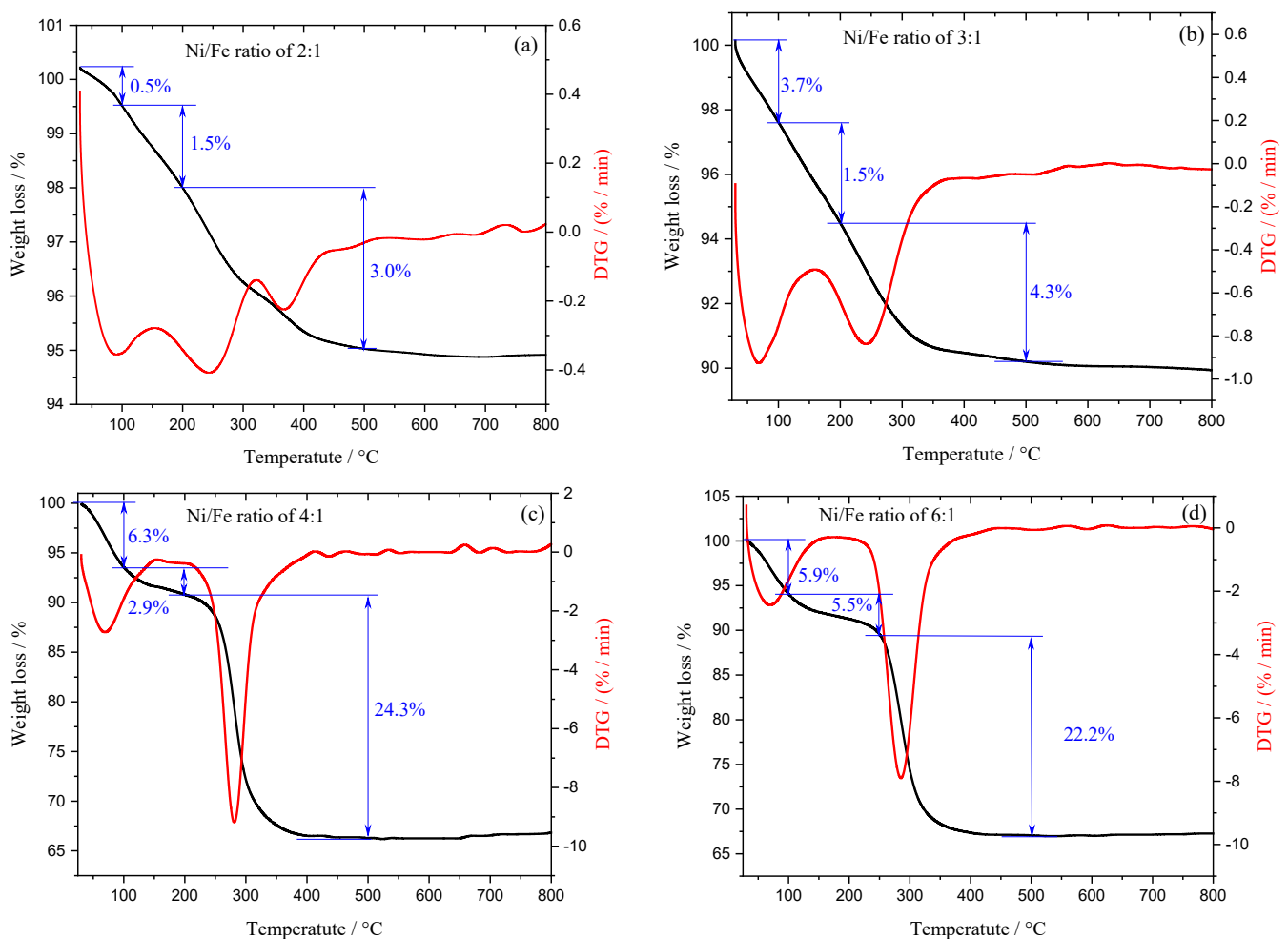


Figure 2. TG and DTG curves of Ni-Fe LDH samples. Ni/Fe ratios of 2 (a), 3 (b), 4 (c) and 6 (d).

3.2. Friction and Wear Performance

Figure 3 provided the variations of the friction coefficient (COF), the average friction coefficient (AFC) and the wear scar diameter (WSD) of GTL base oil with load, as well as the variations of COF, AFC and WSD of GTL base oil with Ni-Fe ratio and concentration. The lubricating performance of GTL base oil was tested under 200–600 N in Figure 3a,b. All the COF curves of GTL base oil remained stable under the loads of 200, 300, 400, 500, and 600 N. As the load increases, the AFC decreases and then increases, and the WSD gradually increases from 0.54 mm to 0.91 mm. This is because, the increase in load will result in the lubrication state in the metal-to-metal contact zone transition from boundary lubrication to mixed lubrication according to the Stribeck curve. In order to study the tribological performance of Ni-Fe LDHs, the variations of COF, AFC and WSD of GTL base oil with different Ni-Fe ratio and concentration are shown in Figure 3c–j. It can be seen that as the Ni-Fe ratio increases from 2:1 to 6:1, the AFC and WSD of GTL base oil with Ni-Fe LDHs presents similar variations. As the concentration of Ni-Fe LDHs increased from 0 mg/mL to 0.3 mg/mL, the AFC and WSD decreases, while the concentration of Ni-Fe LDHs increased from 0.4 mg/mL to 0.5 mg/mL, the AFC and WSD increases. At the same concentration (0.3 mg/mL), the AFC and WSD of Ni-Fe LDH (Ni/Fe ratio of 6) are the smallest, reducing by 51.3% and 30.8%, respectively, which shows the best lubricating performance.

In order to better understand the wear characteristic of GTL base oil before and after enhanced with 0.3 mg/mL Ni-Fe LDH with Ni/Fe ratio of 6, wear surface morphology was observed by WLI. The steel ball with wear scars was firstly cleaned by ultrasonic with ethanol. A wear scar with the wear volume of $3,076,504 \mu\text{m}^3$, surface roughness (Ra) value of $3.0 \mu\text{m}$ and the average wear scar depth of $38 \mu\text{m}$ were formed for GTL based oil as seen in Figure 4a–c. It was obvious that the wear volume, the surface roughness and the average depth of the wear marks on the steel balls differed when using GTL base oil + 0.3 mg/mL Ni-Fe LDH (Ni/Fe ratio of 6). The obtained results showed that GTL based oil + 0.3 mg/mL Ni-Fe LDH with Ni/Fe ratio of 6 which had smaller AFC and WSD displayed the wear scar with lower wear volume, surface roughness and average wear scar depth (see Figure 4d–f). In a comparison, the wear volume, surface roughness and average wear scar depth decreased 78.4%, 6.7% and 50.0%, respectively. It was believed that the effects of Ni-Fe LDH alleviated adhesion.

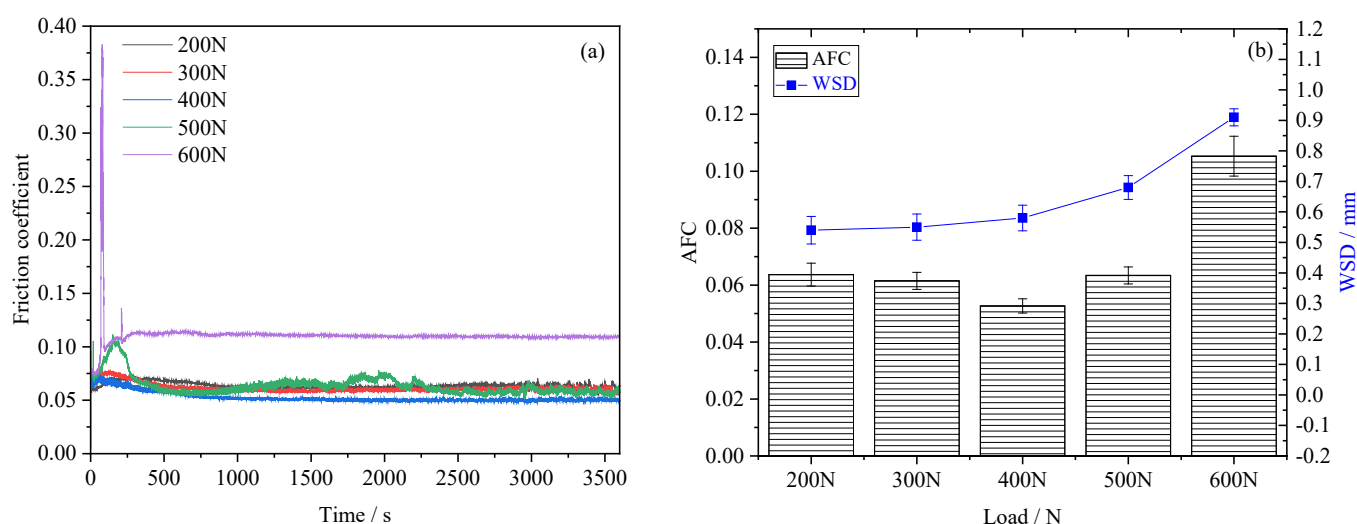


Figure 3. Cont.

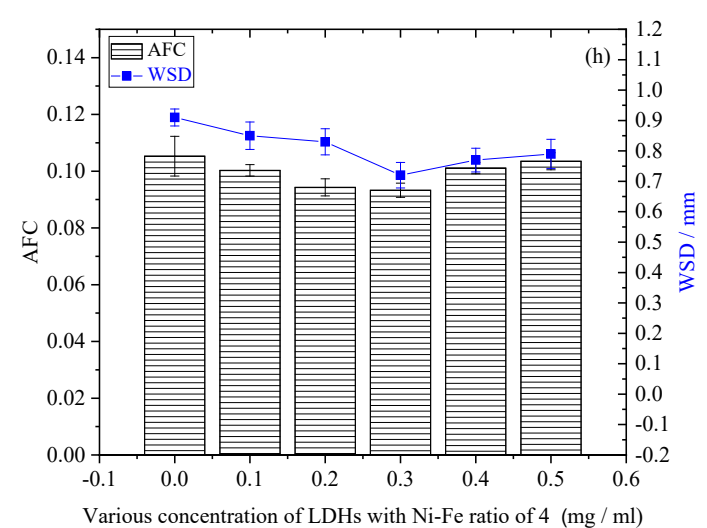
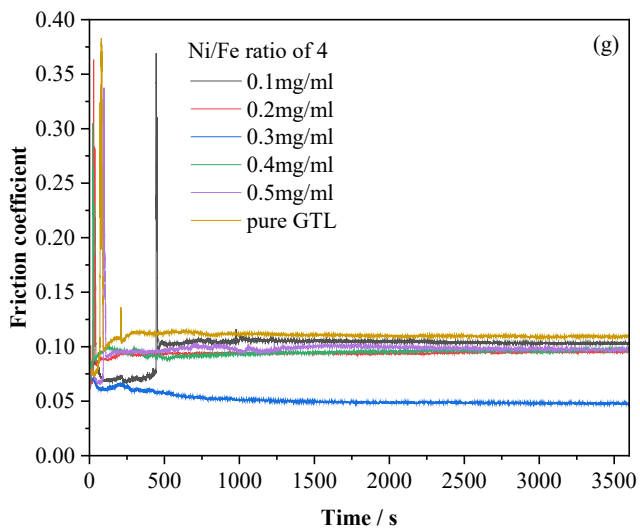
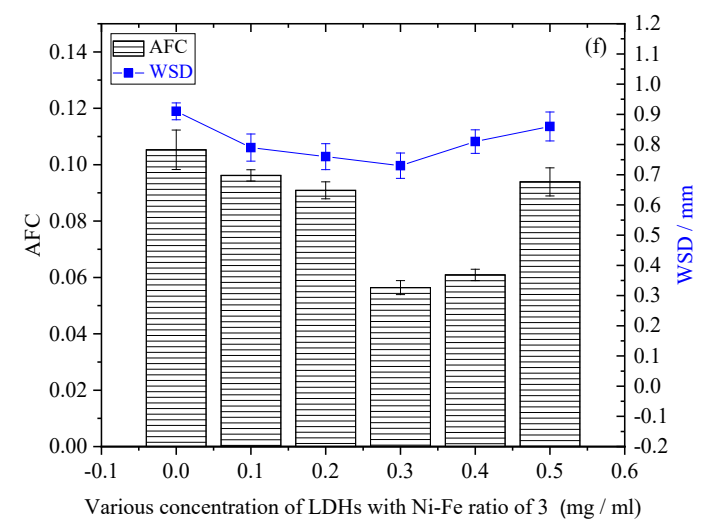
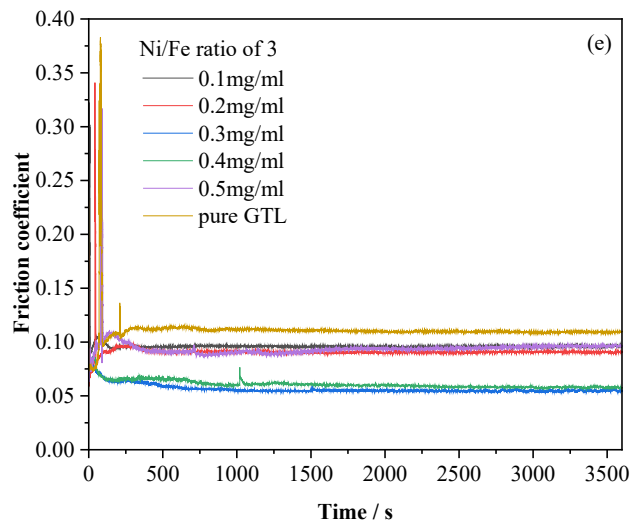
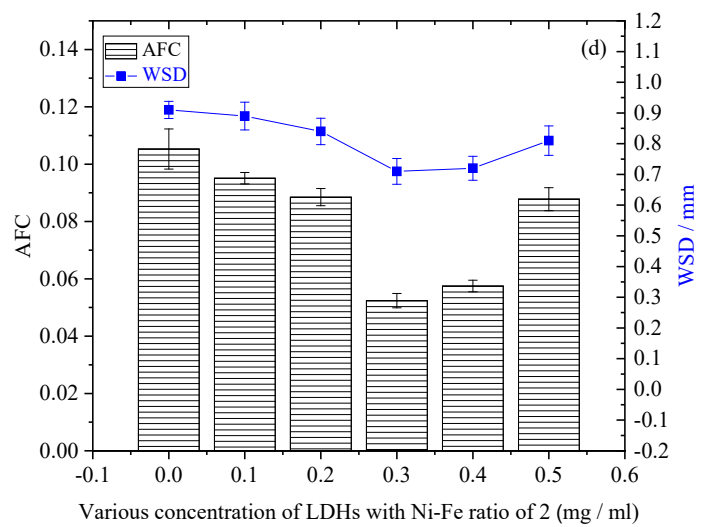
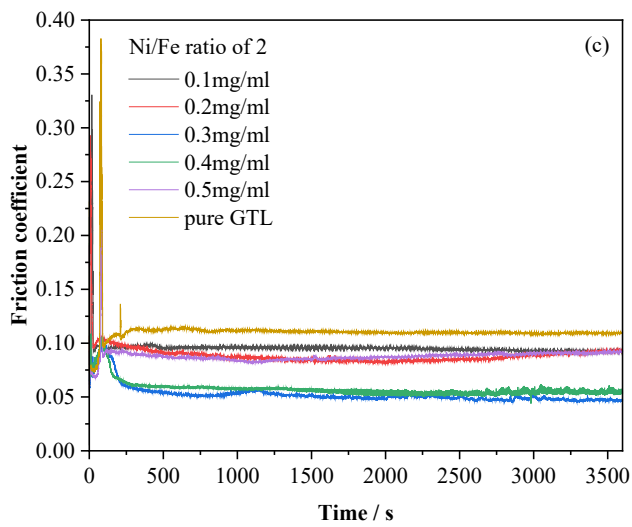


Figure 3. Cont.

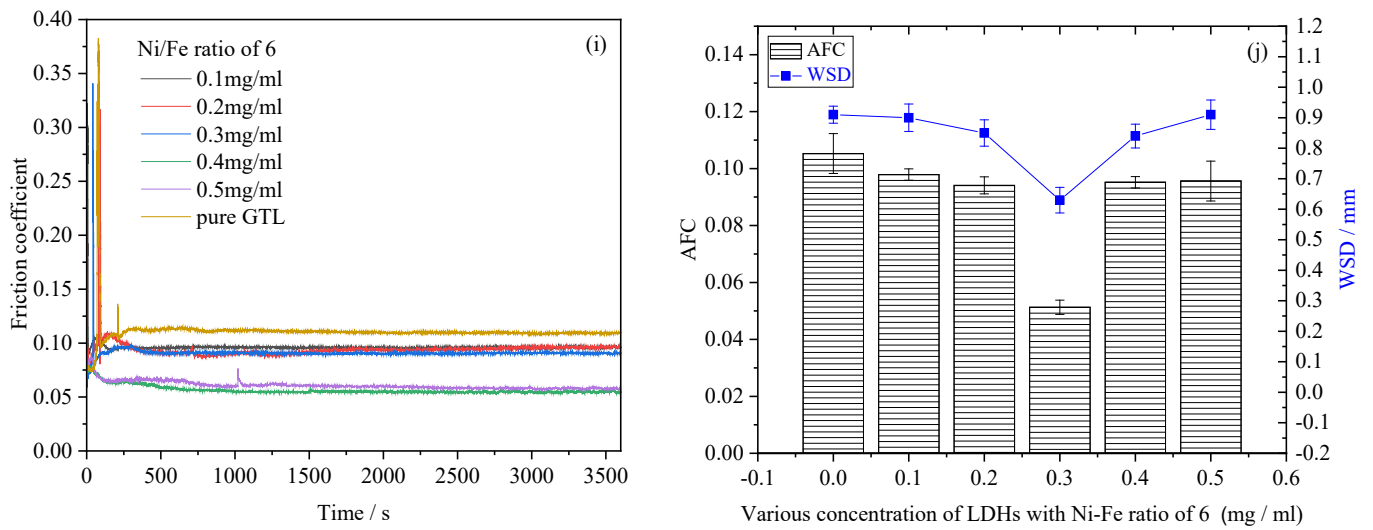


Figure 3. Tribological performance of Ni-Fe LDHs. (a,b) variations of COF, AFC and WSD of GTL base oil with load (60 min, RT, 1200 rpm), (c–j) variations of COF, AFC and WSD of GTL base oil with Ni-Fe ratio and concentration (600 N, 60 min, RT, 1200 rpm).

3.3. Worn Surface Analysis

In order to investigate the lubrication effect of Ni-Fe LDHs as lubricant additives on the contact area of steel balls during the friction test, the morphology of the wear marks was observed using an optical microscope and a scanning electron microscope equipped with an EDS detector to detect the distribution of the corresponding elements on the wear mark surface after the friction test. As shown in Figure 5, deep grooves and flaking pits were observed on the wear surfaces lubricated with GTL base oil. The elements C, O and Fe were detected on the surface of the wear marks, with O coming from air and C from thermal decomposition of GTL base oil.

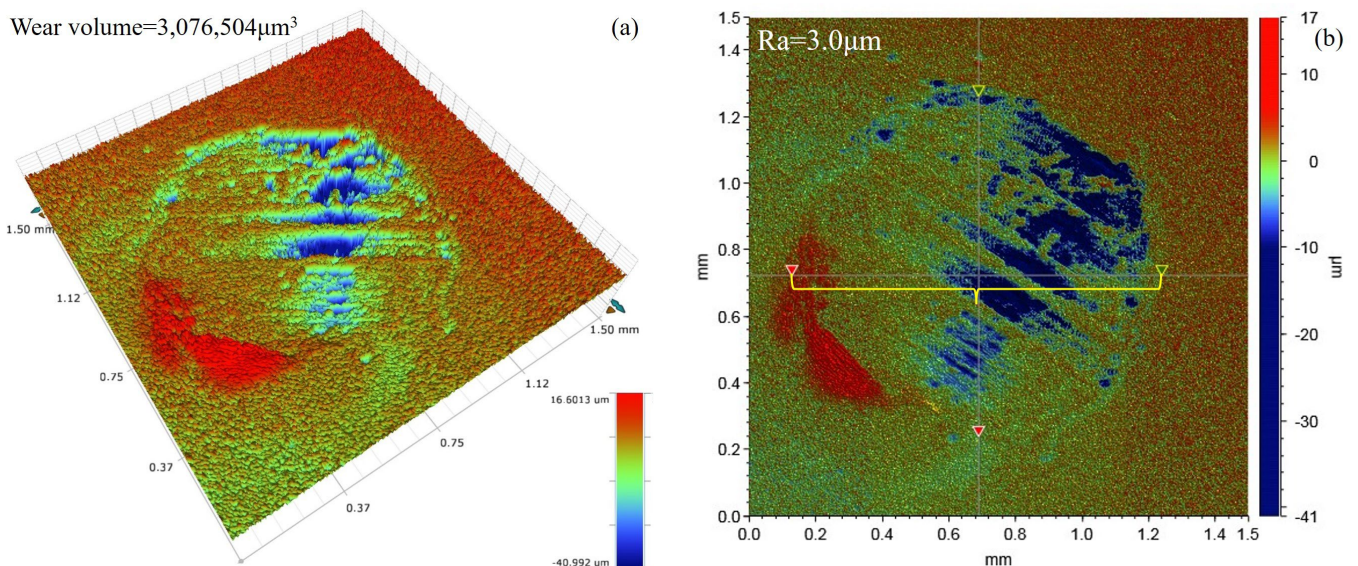


Figure 4. Cont.

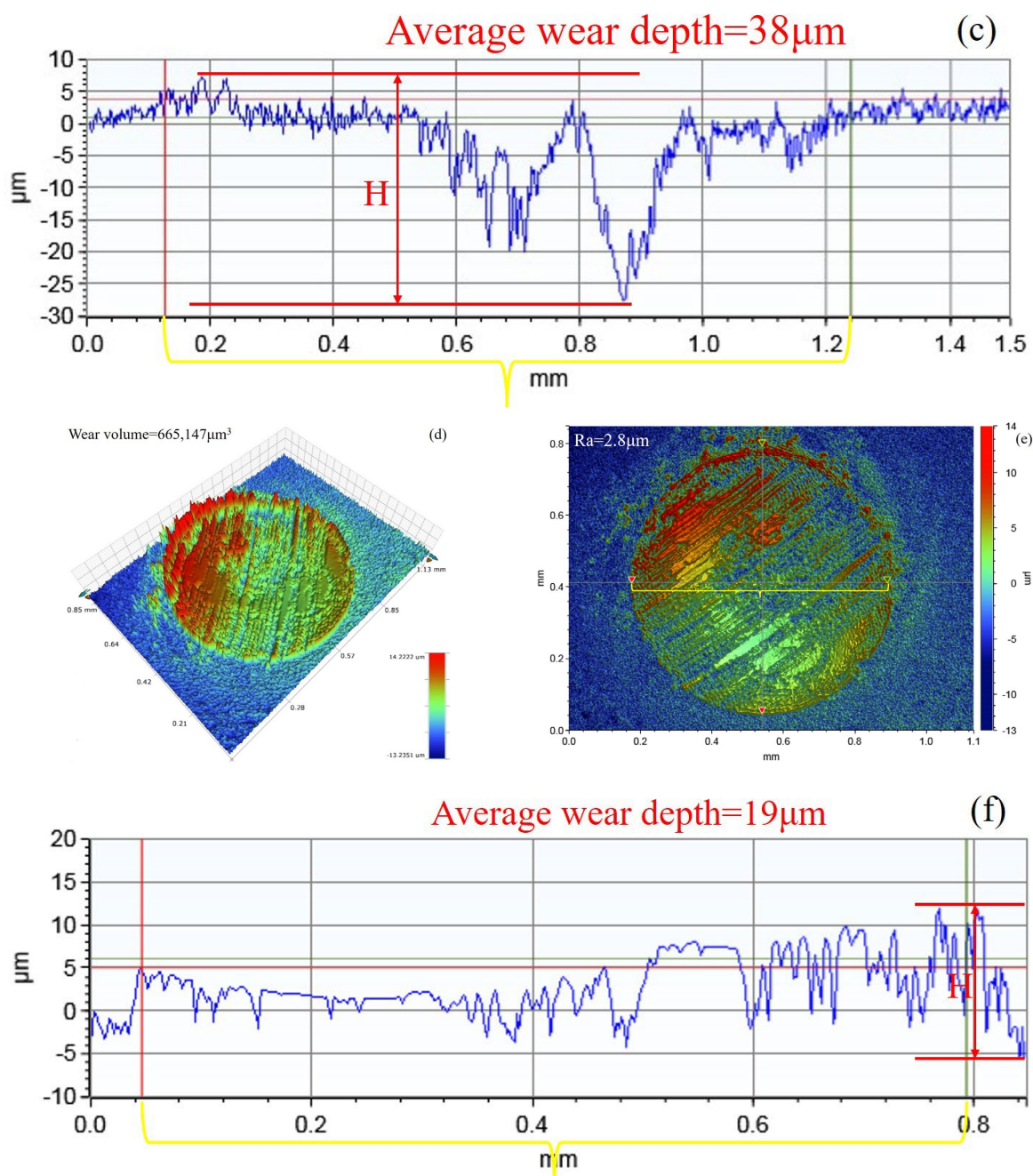


Figure 4. 3D morphology and average depth of steel ball wear scar surfaces, (a–c) lubricated by GTL base oil, (d–f) lubricated by GTL base oil + 0.3 mg/ml Ni–Fe LDH with Ni/Fe ratio of 6.

After that, the morphology and the corresponding element distribution on the wear scar surface lubricated by GTL base oil + 0.3 mg/mL Ni-Fe LDH with Ni/Fe ratio of 6 is shown in Figure 6 to prove the lubricating effect of Ni-Fe LDHs on the two sliding surfaces. It can be readily found that the worn surface looks very smooth with little visible wear after adding the Ni-Fe LDHs into GTL base oil. The C, O, Fe, and Ni four kinds of elements were detected on the wear scar surface. In addition, after adding Ni-Fe LDHs, elemental O is obviously increased compared with the GTL base oil, which certifies that the wear scar surface of the steel ball produced a tribofilm after the addition of Ni-Fe LDHs. The detected Ni elements were primarily from the Ni-Fe LDHs. Additionally, Ni observed on the wear scar surface, indicating that the adsorption of Ni-Fe LDHs occurred on the surface of the bottom balls from tests.

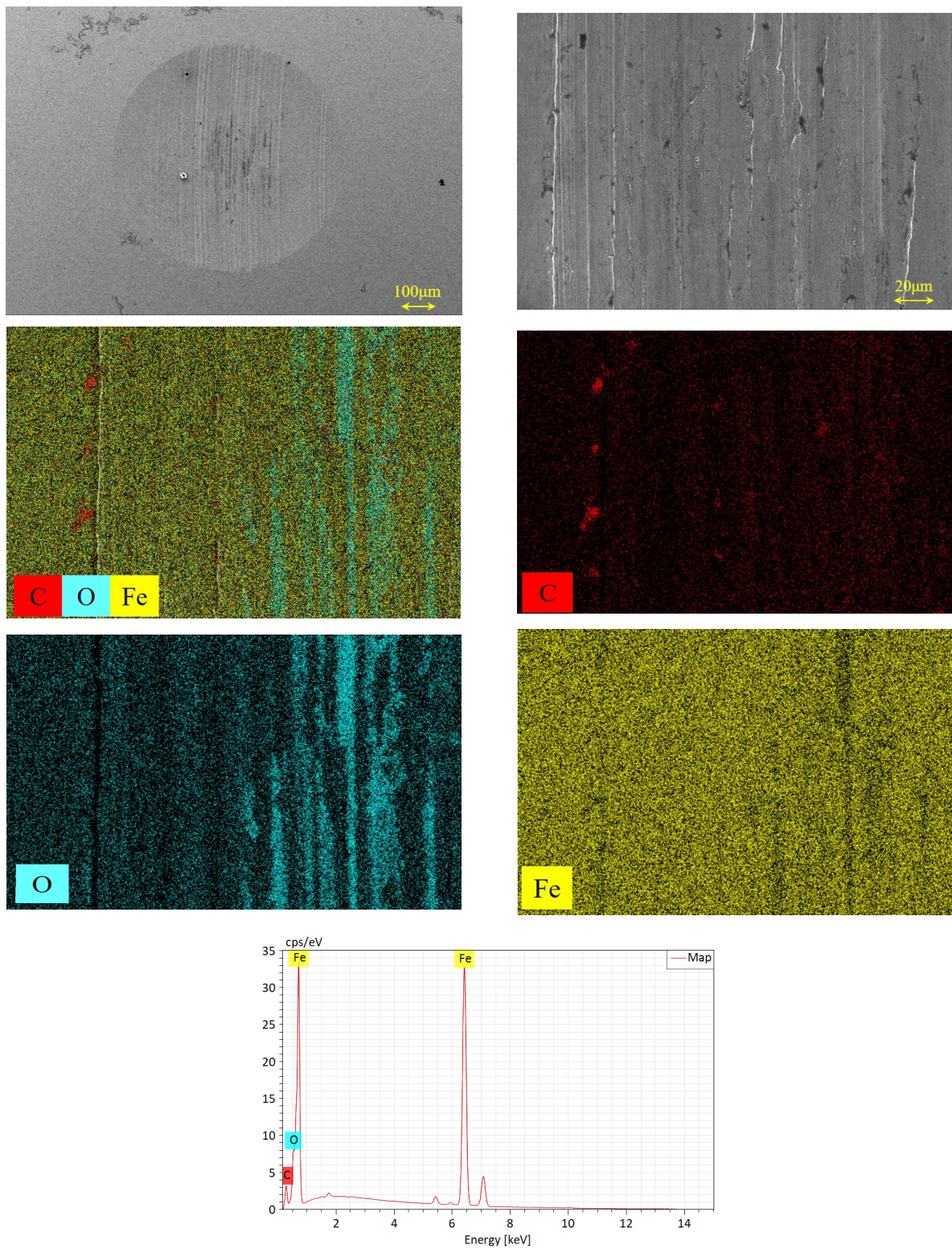


Figure 5. SEM images and EDS mapping of worn surface of steel ball lubricated by GTL base oil.

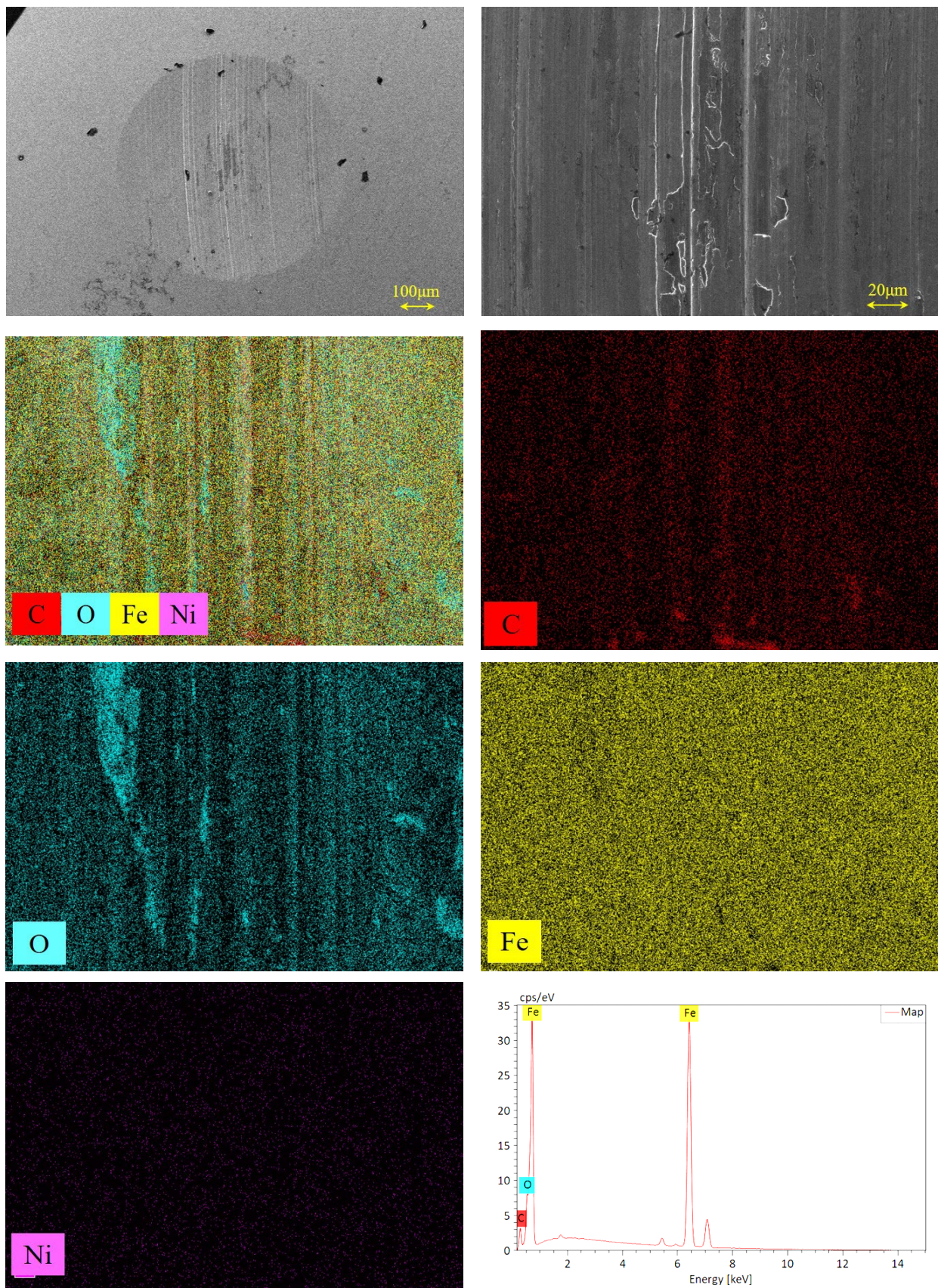


Figure 6. SEM images and EDS mapping of worn surface of steel ball lubricated by GTL base oil + 0.3 mg/mL Ni-Fe LDH with Ni/Fe ratio of 6.

To further clarify the composition of the tribochemical or adsorption film, the XPS was used to characterize the contact area on the steel ball worn surface. Figure 7 presents that the survey spectra of the steel ball worn surface and the high resolution spectra of C 1s, Fe 2p, Ni 2p, O 1s. According to Figure 7a, the peaks of C 1s, Fe 2p, and O 1s were founded on the survey spectrum lubricated by GTL base oil. While the peaks of C 1s, Fe 2p, and O 1s and Ni 2p were founded on the survey spectrum lubricated by GTL base oil + 0.3 mg/mL Ni-Fe LDH with Ni/Fe ratio of 6. According to Figure 7b, the peaks of element C near 284.63 and 288.78 eV respectively assigned to C=C and C=O, suggesting that some carbon-containing material on the worn surface originates from thermal cracking and coke deposition of the GTL base oil. In Figure 7c, the subpeak at a higher binding energy (725.13 eV) is attributed to Fe_3O_4 , while the lower subpeak (710.83 eV) is contributed by Fe_2O_3 . The Ni 2p spectrum (Figure 7d) with subpeak at 854.88 eV suggests that Ni exists as NiO on the rubbing surface by tribochemical reaction. In Figure 7e, the peaks near 529.63 eV and 531.43 eV of the O 1s spectrum lubricated by GTL base oil + 0.3 mg/mL Ni-Fe LDH with Ni/Fe ratio of 6 attributed to the NiO and iron oxides, respectively. While the peak near 531.88 eV of the O 1s spectrum lubricated by GTL base oil attributed to the iron oxides. Therefore, it is justified to conclude that the tribofilm deposited on the worn surface of the steel ball uniformly and densely, which was primarily made up of iron oxides and NiO, proving that Ni-Fe LDHs indeed benefited to enhance the tribological behavior of GTL base oil.

3.4. Lubrication Mechanism of Ni-Fe LDH

In this paper, the four-sphere point contact model in contact mechanics is used to investigate the contact stress pattern of a point contact object under pressure in order to assess its tribological behaviour (Figure 8a).

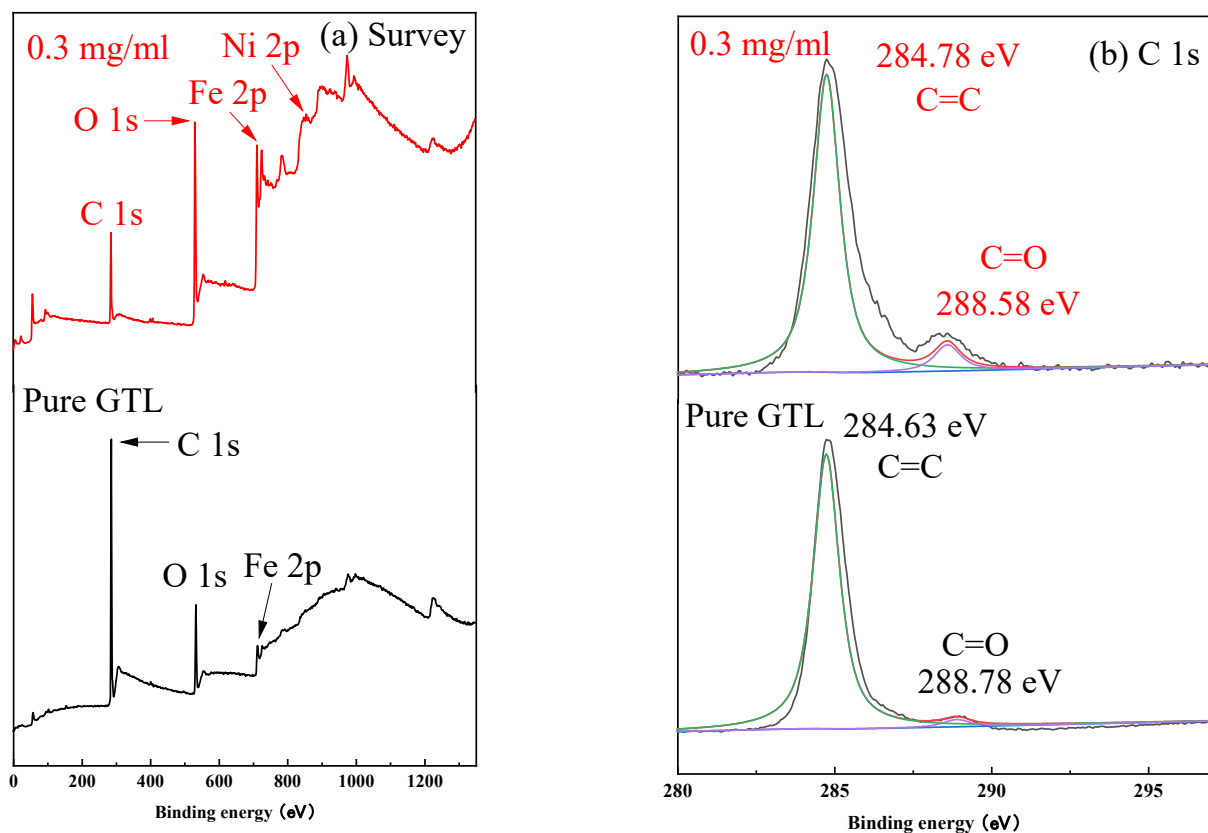


Figure 7. Cont.

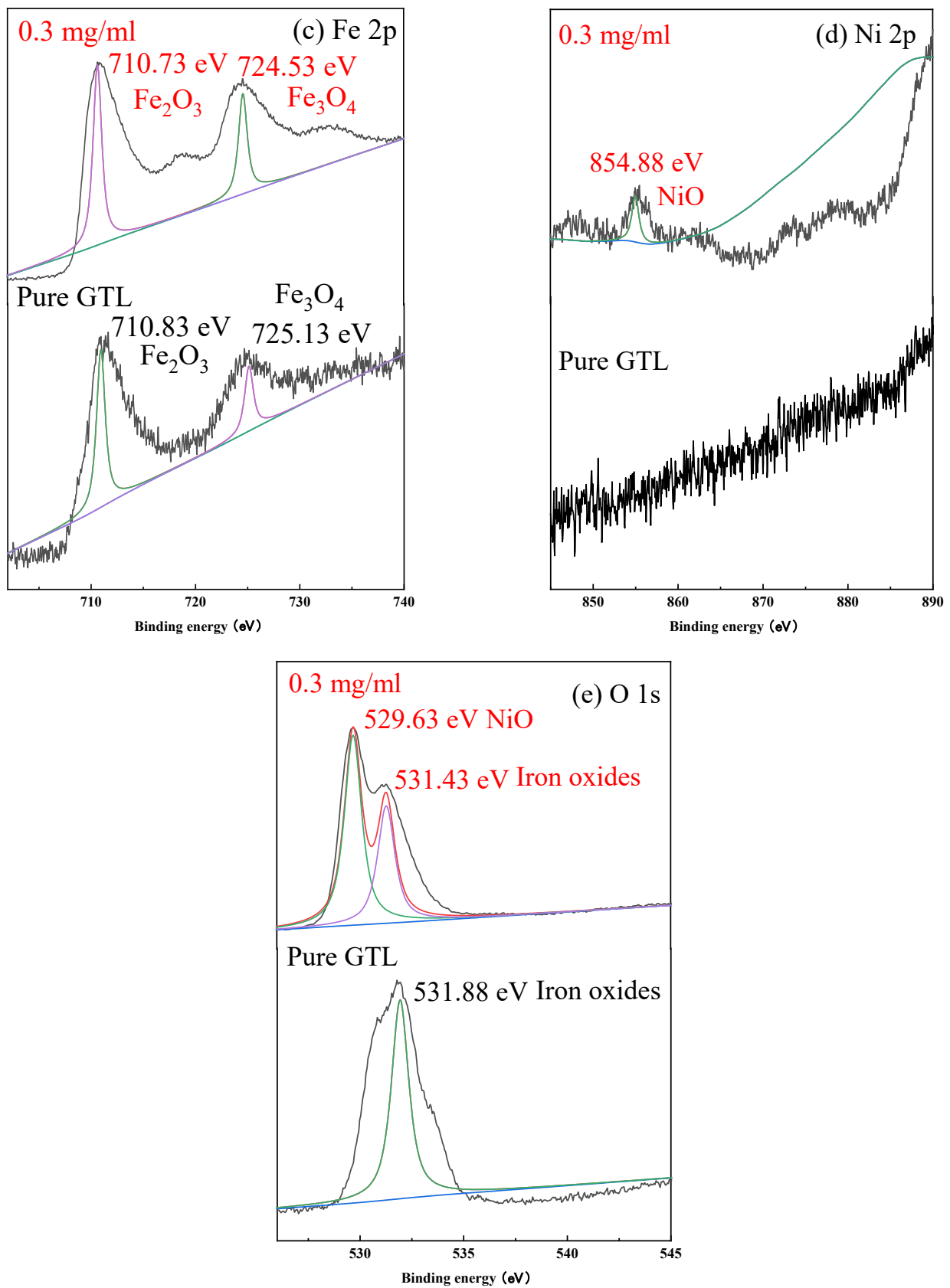


Figure 7. XPS spectrum of steel ball wear spot surface lubricated by GTL base oil and GTL base oil + 0.3 mg/ml Ni–Fe LDH with Ni/Fe ratio of 6. (a) XPS survey spectra, (b) C 1s, (c) Fe 2p, (d) Ni 2p, (e) O 1s.

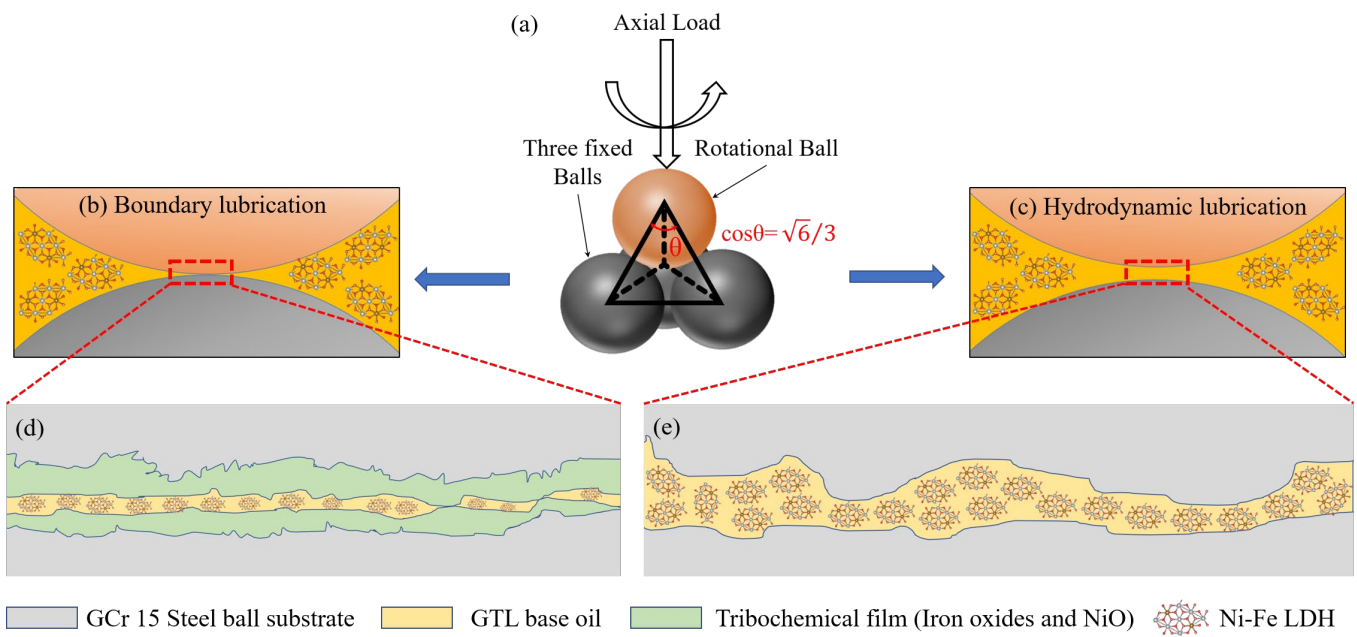


Figure 8. Schematic diagrams of lubrication mechanism for GTL base oil enhanced with Ni-Fe LDH with Ni/Fe ratio of 6: (a) schematic illustration of the four-sphere point contact model, (b,d) boundary lubrication between two sliding surfaces of a solid rough peaks and ridges, (c,e) hydrodynamic lubrication in the area of fluid contact.

The rotating upper ball was located on a spindle, whereas the lower three stationary balls were fixed in an oil cup. Based on Hertz contact theory, the maximum contact pressure at the center of the circular contact area is given by:

$$q_{max} = \frac{3p}{2\pi a^2} \tag{1}$$

$$a = \left(\frac{3}{4} \times \frac{pR'}{E^*} \right)^{\frac{1}{3}} \tag{2}$$

Herein, q_{max} is the maximum contact stress between the steel balls, p is the effective load, a is the radius of the steel balls contact area, E^* is the equivalent Young’s modulus, R' is the comprehensive radius. p , E^* , and R' are defined as:

$$w = 3p \cos \theta \tag{3}$$

$$\frac{1}{R'} = \frac{1}{R_{above}} + \frac{1}{R_{below}} \tag{4}$$

$$E^* = \left(\frac{1 - \nu_{above}^2}{E_{above}} + \frac{1 - \nu_{below}^2}{E_{below}} \right)^{-1} \tag{5}$$

In this model contact, the polygon of the steel ball friction pair is a regular triangular pyramid with four ball centers as vertices, according to which $\cos \theta = \sqrt{6}/3$, and the effective load (p) of every steel ball is calculated by the equation (Equation (3)), where w is the total load, R_{above} is the radius of the rotating upper ball, R_{below} are the radii of the lower three stationary balls, ν_{above} and E_{above} are Poisson’s ratio and Young’s modulus of the rotating upper ball, respectively, ν_{below} and E_{below} are Poisson’s ratio and Young’s modulus of the lower three stationary balls, respectively.

The effective load of each ball is estimated to be 245 N for the total applied load of 600 N and the maximum contact pressure calculated by the Hertz contact stress formula (Equations (1) and (2)) was 3.51 GPa.

For further understanding of the lubrication state between friction pairs and to investigate the tribological properties of Ni-Fe LDH in GTL base oil, the thickness of the lubricating film (h_{min}) was calculated from the Hamrock-Dowson equation (Equation (6)) [30–32]:

$$h_{min} = 3.63 \frac{G^{0.49} U^{0.68} R'}{W^{0.073}} \left(1 - 0.61e^{-0.68k}\right) \quad (6)$$

where $G = \alpha E'$, $U = \eta_0 u / E' R'$, $W = p / E' R'^2$, $k = 1.03(R_y / R_x)^{0.64} = 1.03$ were dimensionless material parameter, dimensionless speed parameter, dimensionless load parameter, ellipticity parameter, respectively. α and η_0 were the viscosity-pressure coefficient and the dynamic viscosity at 25 °C of GTL base oil + 0.3 mg/mL Ni-Fe LDH with Ni/Fe ratio of 6, respectively. u (0.461 m/s) was the relative sliding velocity of the two friction pairs, k was the ellipticity parameter, $E' = 2E^*$ was the effective modulus of elasticity.

Here, the minimum oil film thickness (h_{min}) between the two friction pairs was 1.306 μm . The lubrication state under the four ball experiment could be subsequently classified in accordance with the relationship between the film thickness and surface roughness as follows equation (Equation (7)):

$$\lambda = \frac{h_{min}}{\sqrt{\sigma_1^2 + \sigma_2^2}} \quad (7)$$

where σ_1 (2.8 μm) and σ_2 (2.8 μm) are the surface roughness of the worn area of the upper rotating ball and the lower stationary ball, respectively. This showed that λ is about 2.56 for GTL base oil + 0.3 mg/mL Ni-Fe LDH with Ni/Fe ratio of 6, indicating that the contact area is in a mixed lubrication state which is an intermediary condition between boundary lubrication (Figure 8b) and hydrodynamic lubrication (Figure 8c) [32,33].

Boundary lubrication occurs mainly between two sliding surfaces of a solid rough peaks and ridges (Figure 8d). During the collision close to the cusp, the obvious microscopic fold structure is firstly destroyed under high contact pressure. At the same time, a large number of ultrathin Ni-Fe LDH nanosheets are formed. To some extent, the possibility of direct contact of Ni-Fe LDH nanosheets with sliding solid surfaces is greatly increased. During violent friction, the ultrathin Ni-Fe LDH nanosheets physically hinder the direct collision of the pointed surface in the middle of the contact zone [33]. As sliding proceeds, the physically adsorbed film ruptures under harsh conditions. At this point, the gradual generation of heat, plastic deformation and defects on the worn surface also provide an environment for the subsequent ternary chemical reaction [29]. The ternary chemical reaction between the Ni-Fe LDH additive and the surface of the sliding steel ball generates a new relatively dense ternary protective film, which has better mechanical properties, and can greatly prevent scuffing and protect the solid surfaces from severe collisions.

At the same time, hydrodynamic lubrication occurs mainly in the area of fluid contact (Figure 8e). The dynamic pressure effect caused by the relatively rapid movement of the friction partner also produces a film of hydrodynamic lubrication between the two friction partners. In hydrodynamic lubrication, this film completely separates the concave and convex peaks, thus reducing friction and wear between the balls.

4. Conclusions

In this paper, some kinds of Ni-Fe LDH powders with various Ni/Fe ratio were synthesized via a cost-effective room-temperature co-precipitation process, and its lubricating performance as an oil-based additive in steel–steel contact was studied. It shows that the Ni/Fe ratio of Ni-Fe LDH had a remarkable influence on the lubricating performance improvement of GTL base oil. At the same concentration (0.3 mg/mL), the Ni-Fe LDH with Ni/Fe ratio of 6 was demonstrated to exhibit the best lubricating performance and the AFC, WSD, the wear volume, surface roughness and average wear scar depth decreased 51.3%, 30.8%78.4%, 6.7% and 50.0%, respectively. The lubrication mechanisms are summarized as follows. (1) As a result of the benefit of nanoscale size and layered structure, the

microstructure of Ni-Fe LDH is broken down under the action of high applied pressure at the initial stage, producing a mass of ultrathin Ni-Fe LDH nanosheets, which form a physical adsorption film on the worn surface of the steel ball, polishing and mending the microbulges of worn surface and the defects resulted from harsh friction. (2) As friction proceeds, the physical film described above ruptures under harsh conditions. As a result of heating, plastic deformation and peeling of the worn surface of the steel ball, a new triple chemical film consisting of iron and nickel oxides with better mechanical properties is produced and gradually replaces the physical adsorption film, thus resisting scratches and protecting the solid surface from extremely severe impacts.

Author Contributions: Investigation, S.X., X.Z., H.B., Q.Z. and Y.H.; resources, S.X. and Q.Z.; methodology and validation, S.X., X.Y. and Q.T.; visualization and formal analysis, S.X., P.L. and B.H.; supervision, S.X., Q.Z., X.D. and Y.H.; writing—original draft preparation, S.X., S.L., Q.Z. and S.W.; writing—review and editing, S.X., X.Z., Q.Z., X.Y., P.L., Q.T., X.D. and Y.H. All authors have read and agreed to the published version of the manuscript.

Funding: This research was funded by Science and Technology Research Program of Chongqing Municipal Education Commission, grant number KJZD-K202212905 and Natural Science Foundation of Chongqing, grant number cstc2019jcyj-msxmX0453.

Data Availability Statement: The original contributions presented in the study are included in the article, further inquiries can be directed to the corresponding author.

Conflicts of Interest: The authors declare no conflicts of interest.

References

1. Duan, L.; Li, J.; Duan, H. Nanomaterials for lubricating oil application: A review. *Friction* **2023**, *11*, 647–684. [[CrossRef](#)]
2. Jiang, H.; Hou, X.; Qian, Y.; Liu, H.; Ahmed Ali, M.K.; Dearn, K.D. A tribological behavior assessment of steel contacting interface lubricated by engine oil introducing layered structural nanomaterials functionalized by oleic acid. *Wear* **2023**, *524–525*, 204675. [[CrossRef](#)]
3. Rawat, S.S.; Harsha, A.P.; Khatri, O.P. Tribological Investigations of Two-Dimensional Nanostructured Lamellar Materials as Additives to Castor-Oil-Derived Lithium Grease. *J. Tribol.* **2022**, *144*, 091902. [[CrossRef](#)]
4. Singh, A.; Chauhan, P.; Mamatha, T.G. A review on tribological performance of lubricants with nanoparticles additives. *Mater. Today Proc.* **2020**, *25*, 586–591. [[CrossRef](#)]
5. Zhou, C.; Li, Z.; Liu, S.; Zhan, T.; Li, W.; Wang, J. Layered double hydroxides for tribological application: Recent advances and future prospective. *Appl. Clay Sci.* **2022**, *221*, 106466. [[CrossRef](#)]
6. Luo, J.; Liu, M.; Ma, L. Origin of friction and the new frictionless technology—Superlubricity: Advancements and future outlook. *Nano Energy* **2021**, *86*, 106092. [[CrossRef](#)]
7. Chen, W.; Feng, Y.; Wan, Y.; Zhang, L.; Yang, D.; Gao, X.; Yu, Q.; Wang, D. Investigation on anti-wear and corrosion-resistance behavior of steel-steel friction pair enhanced by ionic liquid additives under conductive conditions. *Tribol. Int.* **2023**, *177*, 108002. [[CrossRef](#)]
8. Bowden, F.P.; Tabor, D. *The Friction and Lubrication of Solids*; Oxford University Press: Oxford, UK, 2001.
9. Li, S.; Bhushan, B. Lubricating performance and mechanisms of Mg/Al-, Zn/Al-, and Zn/Mg/Al-layered double hydroxide nanoparticles as lubricant additives. *Appl. Surf. Sci.* **2016**, *378*, 308–319. [[CrossRef](#)]
10. Gong, H.; Yu, C.; Zhang, L.; Xie, G.; Guo, D.; Luo, J. Intelligent lubricating materials: A review. *Compos. Part B Eng.* **2020**, *202*, 108450. [[CrossRef](#)]
11. Xia, L.; Long, J.; Zhao, Y.; Wu, Z.; Dai, Z.; Wang, L. Molecular Dynamics Simulation on the Aggregation of Lubricant Oxidation Products. *Tribol. Lett.* **2018**, *66*, 104. [[CrossRef](#)]
12. Sulima, S.I.; Bakun, V.G.; Chistyakova, N.S.; Larina, M.V.; Yakovenko, R.E.; Savost'yanov, A.P. Prospects for Technologies in the Production of Synthetic Base Stocks for Engine Oils (A Review). *Pet. Chem.* **2021**, *61*, 1178–1189. [[CrossRef](#)]
13. Paul, G.; Hirani, H.; Kuila, T.; Murmu, N.C. Nanolubricants dispersed with graphene and its derivatives: An assessment and review of the tribological performance. *Nanoscale* **2019**, *11*, 3458–3483. [[CrossRef](#)] [[PubMed](#)]
14. Jin, B.; Chen, G.; He, Y.; Zhang, C.; Luo, J. Lubrication properties of graphene under harsh working conditions. *Mater. Today Adv.* **2023**, *18*, 100369. [[CrossRef](#)]
15. Wang, Q.; Hou, T.; Wang, W.; Zhang, G.; Gao, Y.; Wang, K. Tribological behavior of black phosphorus nanosheets as water-based lubrication additives. *Friction* **2022**, *10*, 374–387. [[CrossRef](#)]
16. Tang, G.; Wu, Z.; Su, F.; Wang, H.; Xu, X.; Li, Q.; Ma, G.; Chu, P.K. Macroscale Superlubricity on Engineering Steel in the Presence of Black Phosphorus. *Nano Lett.* **2021**, *21*, 5308–5315. [[CrossRef](#)] [[PubMed](#)]
17. Chen, H.; Xiao, G.; Chen, Z.; Yi, M.; Zhang, J.; Li, Z.; Xu, C. Hexagonal boron nitride (h-BN) nanosheets as lubricant additive to 5CB liquid crystal for friction and wear reduction. *Mater. Lett.* **2022**, *307*, 131007. [[CrossRef](#)]

18. An, L.; Yu, Y.; Bai, C.; Bai, Y.; Zhang, B.; Gao, K.; Wang, X.; Lai, Z.; Zhang, J. Simultaneous production and functionalization of hexagonal boron nitride nanosheets by solvent-free mechanical exfoliation for superlubricant water-based lubricant additives. *NPJ 2d Mater. Appl.* **2019**, *3*, 28. [[CrossRef](#)]
19. Xiang, S.; Long, X.; Zhang, Q.; Ma, P.; Yang, X.; Xu, H.; Lu, P.; Su, P.; Yang, W.; He, Y. Enhancing Lubricating performance of Calcium Sulfonate Complex Grease Dispersed with Two-Dimensional MoS₂ Nanosheets. *Lubricants* **2023**, *11*, 336. [[CrossRef](#)]
20. Liu, C.; Meng, Y.; Tian, Y. Potential-Controlled Boundary Lubrication Using MoS₂ Additives in Diethyl Succinate. *Tribol. Lett.* **2020**, *68*, 72. [[CrossRef](#)]
21. Wu, H.; Yin, S.; Du, Y.; Wang, L.; Wang, H. An investigation on the lubrication effectiveness of MoS₂ and BN layered materials as oil additives using block-on-ring tests. *Tribol. Int.* **2020**, *151*, 106516. [[CrossRef](#)]
22. Lu, Z.; Cao, Z.; Hu, E.; Hu, K.; Hu, X. Preparation and tribological properties of WS₂ and WS₂/TiO₂ nanoparticles. *Tribol. Int.* **2019**, *130*, 308–316. [[CrossRef](#)]
23. Wang, C.; Zhang, X.; Jia, W.; Deng, Q.; Leng, Y. Preparation and Tribological Properties of Modified Field's Alloy Nanoparticles as Additives in Liquid Poly- α -olefin Solution. *J. Tribol.* **2019**, *141*, 1. [[CrossRef](#)]
24. Zhou, C.; Li, Z.; Liu, S.; Ma, L.; Zhan, T.; Wang, J. Synthesis of MXene-Based Self-dispersing Additives for Enhanced Tribological Properties. *Tribol. Lett.* **2022**, *70*, 63. [[CrossRef](#)]
25. Miao, X.; Li, Z.; Liu, S.; Wang, J.; Yang, S. MXenes in tribology: Current status and perspectives. *Adv. Powder Mater.* **2023**, *2*, 100092. [[CrossRef](#)]
26. Boidi, G.; de Queiróz, J.C.F.; Profito, F.J.; Rosenkranz, A. Ti₃C₂Tx MXene Nanosheets as Lubricant Additives to Lower Friction under High Loads, Sliding Ratios, and Elevated Temperatures. *ACS Appl. Nano Mater.* **2023**, *6*, 729–737. [[CrossRef](#)]
27. Wang, K.; Wu, H.; Wang, H.; Liu, Y. Superior extreme pressure properties of different layer LDH nanoplatelets used as boundary lubricants. *Appl. Surf. Sci.* **2020**, *530*, 147203. [[CrossRef](#)]
28. Pancrecius, J.K.; Gopika, P.S.; Suja, P.; Ulaeto, S.B.; Gowd, E.B.; Rajan, T.P.D. Role of layered double hydroxide in enhancing wear and corrosion performance of self-lubricating hydrophobic Ni-B composite coatings on aluminium alloy. *Colloids Surf. A Physicochem. Eng. Asp.* **2022**, *634*, 128017. [[CrossRef](#)]
29. Wang, H.; Wang, Y.; Liu, Y.; Zhao, J.; Li, J.; Wang, Q.; Luo, J. Tribological behavior of layered double hydroxides with various chemical compositions and morphologies as grease additives. *Friction* **2021**, *9*, 952–962. [[CrossRef](#)]
30. Wei, X.; Li, W.; Fan, X.; Zhu, M. MoS₂-functionalized attapulgite hybrid toward high-performance thickener of lubricating grease. *Tribol. Int.* **2023**, *179*, 108135. [[CrossRef](#)]
31. Hamrock, B.J.; Dowson, D. Isothermal Elastohydrodynamic Lubrication of Point Contacts: Part II—Ellipticity Parameter Results. *J. Lubr. Technol.* **1976**, *98*, 375–381. [[CrossRef](#)]
32. Liu, Y.; Li, J.; Li, J.; Yi, S.; Ge, X.; Zhang, X.; Luo, J. Shear-Induced Interfacial Structural Conversion Triggers Macroscale Superlubricity: From Black Phosphorus Nanoflakes to Phosphorus Oxide. *ACS Appl. Mater. Interfaces* **2021**, *13*, 31947–31956. [[CrossRef](#)] [[PubMed](#)]
33. Wang, D.; Yang, J.; Wei, P.; Pu, W. A mixed EHL model of grease lubrication considering surface roughness and the study of friction behavior. *Tribol. Int.* **2021**, *154*, 106710. [[CrossRef](#)]

Disclaimer/Publisher's Note: The statements, opinions and data contained in all publications are solely those of the individual author(s) and contributor(s) and not of MDPI and/or the editor(s). MDPI and/or the editor(s) disclaim responsibility for any injury to people or property resulting from any ideas, methods, instructions or products referred to in the content.